Research of characterization of zinc ferrite, titanium dioxide and their composites

Jinlin Yang[1,a], Xingnan HuO[1,b], Zongyu Li[1,c] and Shaojian Ma[1,d]*

College of Resources, Environment and Materials, Guangxi University, Nanning 530004, China

Abstract: In this paper, zinc calcines, sulfuric acid, ferric nitrate nine-hydrate, zinc nitrate hexahydrate, titanium oxide sulfate, sodium hydroxide and ammonia water were selected as raw materials, and the methods of sulfuric acid leaching and chemical coprecipitation were used to prepare purified zinc ferrite, synthetic zinc ferrite, synthetic titanium dioxide and its composite with purified zinc ferrite. And characterized by BET, UV-Vis and FTIR. The results showed that: SO_4^{2-} existed in purified zinc ferrite. Purified zinc ferrite, synthetic zinc ferrite and purchased had different specific surface area, pore volume and average pore size. The specific surface area of synthetic zinc ferrite decreased with the increase of calcination temperature. The three kinds of zinc ferrite had good absorption of ultraviolet light and visible light. Purchased ferric acid had the strongest absorption of UV light and synthetic zinc ferrite had the strongest absorption of visible light, and purified zinc ferrite had the absorption of UV light and visible light between the two. The specific surface area of titanium dioxide prepared by chemical coprecipitation method was greatly affected by calcination temperature. With the increase of calcination temperature, the specific surface area decreased from 123.633 to 28.036$m^2 \cdot g^{-1}$, and the average pore diameter was less affected by calcination temperature. For the zinc ferrite/titanium dioxide composite prepared by chemical coprecipitation method, a certain amount of purified zinc ferrite was added to facilitate the absorption of visible light by titanium dioxide.

1. Introduction

Dye wastewater refers to the wastewater discharged in the process of producing dyes and pigments by nitration and iodination of benzene, toluene and naphthalene as raw materials, and then diazotization, coupling and vulcanization[1-4]. Dye wastewater is characterized by large amount of water, high concentration, complex components, deep chrominance, high content of organic pollutants, large changes in water quality, high biological toxicity, and difficult biodegradation. It belongs to the organic wastewater that is difficult to treat. In recent years, photocatalytic oxidation, a new green treatment method, has attracted more and more attention. As a new environmental purification technology, photocatalysis technology can decompose many organic compounds into inorganic small molecules such as CO^2, H_2O, HX and minerals, so as to effectively degrade pollutants and at the same time be friendly to the environment. Zinc ferrite has a wide application prospect in the field of dye wastewater treatment, due to its unique physical and chemical properties. Meanwhile, titanium dioxide is an excellent semiconductor catalyst, which can mineralize a series of organic pollutants, such as dyes and pesticides, under ultraviolet irradiation[5-8]. Therefore, they are often used as photocatalytic oxidation catalysts. However, there are still many difficulties in the practical application of photocatalysis, such as low stability of catalysts, low quantum efficiency, difficult to play a good photocatalytic effect when used alone, and difficult industrial application due to laboratory preparation problems. In addition, the preparation method of the material will affect its composition, morphology, structure and other physical properties, thus affecting its chemical properties. Therefore, it is of great theoretical significance to select an appropriate preparation method, systematically study the influence law of different preparation conditions on material properties, and explore the relationship between material properties and its structure. In this paper, sulfuric acid leaching and chemical coprecipitation methods were used to prepare purified zinc ferrite, synthetic zinc ferrite, synthetic titanium dioxide and its composite with purified zinc ferrite, and characterized by BET, UV-Vis and FTIR.

2. Sample preparation

2.1 Preparation of purified zinc ferrite

Put 100g zinc calcine into a beaker and added 100ml of 4mol/L sulfuric acid solution, sealed it with plastic wrap. The water bath was heated and stirred for leaching at 80℃, and the stirring speed was 300r/min. Took out the beaker after leaching for 2 hours, the supernatant was poured out after cooling, filtered and fully washed. After the filter cake was dried, it was pulverized, screened and reduced for sample preparation. The obtained sample is denoted as PZ.

[a]email: 1915392020@st.gxu.edu.cn, [b]email: 2215394007@st.gxu.edu.cn
[c]email: 2215394012@st.gxu.edu.cn
*Correspondence author: [d]email: 1615391004@alu.gxu.edu.cn

2.2 Preparation of synthetic zinc ferrite

Weighed a certain amount of ferric nitrate nine-hydrate and zinc nitrate hexahydrate at the amount of substance ratio of 2:1 and dissolved them in a beaker. Adjusted the pH value of the solution to 10 with sodium hydroxide, and then stood for 12h after magnetic stirring. When obvious delamination occurred, the supernatant was poured away, and the supernatant was fully washed with ultra-pure water. The obtained precipitation was placed in the oven at 80℃ to get the precursor of zinc ferrite. Transferred it to the crucible, put it in the box-type resistance furnace for calcining, calcination temperature of 400℃, 500℃, 600℃, 700℃, after holding for 2h, took out the sample for grinding, screening, shrinkage sampling. The obtained samples are denoted SZ400, SZ500, SZ600 and SZ700.

2.3 Preparation of synthetic titanium dioxide

Added 30g of titanium oxide sulfate into 200ml of ultra-pure water, stirred magnetically at 60℃ until the solution was clear, then added 45ml of concentrated ammonia water, transferred the beaker to a water bath at 60℃, continued to stir at 500r/min for 40min, and then vacuumed filter to fully wash, and put the filter cake in the oven for dehydration and drying to obtain titanium dioxide precursor. Transferred it to the crucible and put it into the box-type resistance furnace for calcining at the temperature of 300℃, 400℃, 500℃ and 600℃, respectively. After holding for 2h, it was taken out for grinding, screening and sample reduction. The obtained samples are denoted as T300, T400, T500, T600 and T700.

2.4 Preparation of zinc ferrite/titanium dioxide composite

Added 30g of titanium oxide sulfate into 200ml of ultra-pure water, stirred the solution magnetically at 60℃ until the solution was clarified, then added a certain amount of purified zinc ferrite, and then added 45ml of concentrated ammonia water. Transferred the mixture to a water bath at 60℃ and stirred it at 500r/min for 40min to obtain a white thick mixed solution. Then the filter cake was drained under vacuum and washed fully. The filter cake was dehydrated and dried in the oven to obtain the zinc ferrite/titanium dioxide precursor. Transferred it to the crucible, and put the crucible into the box-type resistance furnace for calcining at 400℃ and 500℃ respectively. After holding for 2h, the crucible was ground, screened and divided for sample preparation. The obtained samples are denoted as T400/PZ (5%), T500/PZ (5%), T500/PZ (10%).

3. Characterization analysis

3.1 BET analysis

The specific surface area and pore size distribution of purified zinc ferrite, synthetic zinc ferrite, purchased zinc ferrite, purified zinc ferrite and titanium dioxide (T600) mixture were analyzed by nitrogen adsorption-desorption. The pore size distribution was fitted by BJH model. Nitrogen adsorption-desorption curves of purified zinc ferrite, synthetic zinc ferrite, purchased zinc ferrite, purified zinc ferrite and titanium dioxide (T600) mixture are shown in Figure 1(a), pore size distribution is shown in Figure 1(b), and specific surface area is shown in Table 1. The specific surface area of titanium dioxide at different calcination temperatures is shown in Table 2.

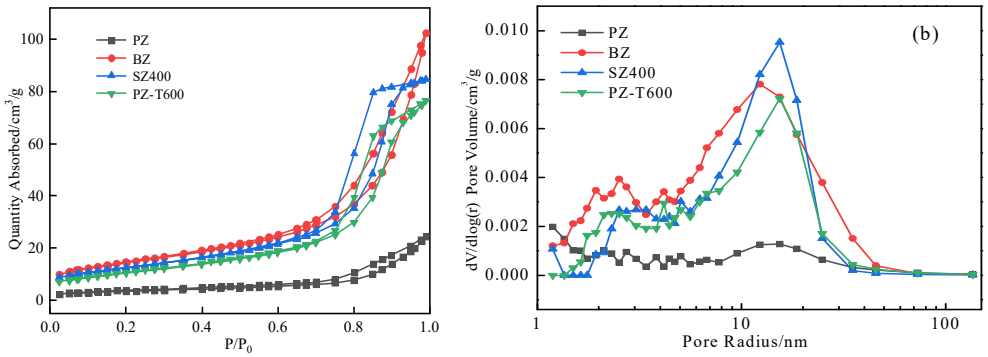

Fig. 1(a) Adsorption desorption curves of different kinds of zinc ferrite; (b) Pore size distribution of different kinds of zinc ferrite

Table 1 Surface parameters of different kinds of zinc ferrite products

Sample	Specific surface area /$m^2 \cdot g^{-1}$	Total pore volume /$cm^3 \cdot g^{-1}$	Average aperture/nm
PZ	9.816	0.033	7.452
BZ	40.470	0.140	7.452
SZ400	35.304	0.126	7.452
SZ500	31.520	0.127	8.522
SZ600	16.657	0.088	8.922
SZ700	10.686	0.055	7.452
Purified zinc ferrite/T600	29.521	0.112	8.529
Purified zinc ferrite/T600	32.617	0.129	7.452
Synthetic zinc ferrite/T600	39.4891	0.185	8.7449

Table 2 Surface parameters of titanium dioxide products calcined at different calcination temperatures

Sample	Specific surface area /$m^2 \cdot g^{-1}$	Total pore volume /$cm^3 \cdot g^{-1}$	Average aperture/nm
T300	123.633	0.249	6.225
T400	79.554	0.181	5.199
T500	78.803	0.204	6.225
T600	48.610	0.157	7.452
T700	28.036	0.115	8.529
T400/PZ（5%）	80.468	0.190	5.439
T500/PZ（5%）	60.372	0.177	6.225
T500/PZ（10%）	61.701	0.155	5.689

It showed from Figure 1(a), the adsorption amount of purified zinc ferrite was the smallest, and the adsorption amount of purchased zinc ferrite was the largest, in terms of the adsorption amount of nitrogen by various zinc ferrites. The adsorption capacity of purified zinc ferrite with titanium dioxide (T600) mixture was comparable to that of synthetic zinc ferrite, but slightly lower than that of purchased zinc ferrite. The results showed that purified zinc ferrite had less pore structure and the number of pores could be improved obviously when it was physically mixed with titanium dioxide. From the type of adsorption isotherm, the adsorption isotherm types of purified zinc ferrite, synthetic zinc ferrite, purchased zinc ferrite, purified zinc ferrite and titanium dioxide (T600) all belong to type IV adsorption isotherm, which indicates that the above adsorption materials may have certain mesopores and macropores. From the hysteresis loop, the purified zinc ferrite and purchased zinc ferrite belonged to the H3 type. From the figure, it showed that that the hysteresis loop isotherm had no obvious saturated adsorption platform, indicating that the pore structure is very incomplete, while the synthesis of zinc ferrite, purification of zinc ferrite and titanium dioxide (T600) mixture belonged to the H2 type, indicating that the pore structure of the two is complex.

It showed from Figure 1(b) that the pore size distribution curve of the purified zinc ferrite, synthetic zinc ferrite, purchased zinc ferrite, purified zinc ferrite and titanium dioxide (T600) mixture were multi-peak type, with the minimum pore size of about 3 nm. Moreover, the pore size distribution characteristics were different and discontinuous, mainly concentrated in the mesoporous range.

From Table 1, it showed that the specific surface areas of the purified zinc ferrite, the purchased zinc ferrite, the synthetic zinc ferrite, and the purified zinc ferrite and titanium dioxide mixture were significantly different. The minimum specific surface area and pore volume of purified zinc ferrite was $9.816 m^2 \cdot g^{-1}$, the maximum specific surface area of purchased zinc ferrite was $40.470 m^2 \cdot g^{-1}$, and the specific surface area of synthetic zinc ferrite decreased with the increase of calcination temperature, ranging from 10.686 to $35.304 m^2 \cdot g^{-1}$. Physical mixing of titanium dioxide (T600), the specific surface area of purified zinc ferrite and titanium dioxide mixture had been greatly improved. However, the specific surface area of the mixture of zinc ferrite (SZ400) and titanium dioxide (T600) and the mixture of zinc ferrite and titanium dioxide (T600) was little changed compared with before mixing. In addition, the specific surface area and pore volume of purified zinc ferrite were far less than the purified zinc ferrite, synthetic zinc ferrite, purified zinc ferrite and titanium dioxide mixture, the reason may be due to the high degree of crystallization of purified zinc ferrite, the closure of micropores on the crystal surface and the adhesion of crystal grains.

It showed from Table 2 that the specific surface area of titanium dioxide decreased with the increase of calcination temperature. The maximum specific surface area was $123.633 m^2 \cdot g^{-1}$ at 300℃, and the minimum specific surface area was $28.036 m^2 \cdot g^{-1}$ at 700℃. The pore volume and average pore diameter were also affected by calcination temperature, and the pore volume was $0.115 \sim 0.249 cm^3 \cdot g^{-1}$, and the average pore diameter was 5.199~8.529nm. The specific surface area of purified zinc ferrite by titanium dioxide doped with different mass fractions changed slightly. When the calcination temperature was 400℃, the specific surface area did not change significantly. When the calcination temperature was 500℃, the specific surface area decreased about $18.431 m^2 \cdot g^{-1}$. The pore volume and average pore diameter did not change significantly.

3.2 UV-Vis analysis

Figure 2(a) shows the UV-Vis spectra of purified zinc ferrite, synthetic zinc ferrite and purchased zinc ferrite. Figure 2(b) shows the UV-Vis spectra of titanium dioxide and purified zinc ferrite/titanium dioxide composite.

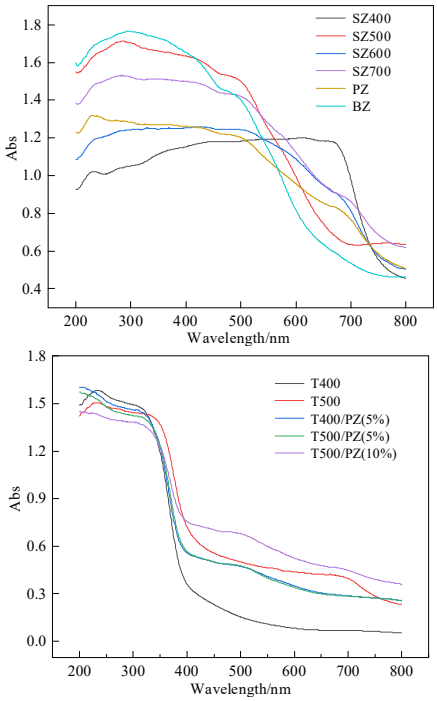

Fig. 2(a) UV-Vis absorption spectra of different zinc ferrite; (b) UV absorption spectra of titanium dioxide and zinc ferrite/titanium dioxide composite

It showed from Figure 2(a) that the three kinds of zinc ferrite had certain absorption to the light with the wavelength of 200~800nm, indicating that the three kinds of zinc ferrite can use visible light. The absorption at 800nm was caused by the transfer transition of the crystal field, the absorption at 400~600nm was due to the metal-metal charge transition, and the absorption below 400nm was due to the Zn-O charge transfer transition and Fe-O charge transfer transition in the zinc ferrite crystal. Comparing the absorption of three kinds of zinc ferrite to ultraviolet light, it can be known that the absorption of ultraviolet light of purchased zinc ferrite is the strongest, and the absorption of ultraviolet light of purified zinc ferrite is at the middle level. The calcination temperature of synthetic zinc ferrite will affect the absorption of ultraviolet light. The absorption of ultraviolet light was the strongest when the calcination temperature was 500℃, while the absorption of ultraviolet light was relatively weak when the calcination temperature was 400℃. By comparing the absorption of three kinds of zinc ferrite to visible light, the synthesis of zinc ferrite is relatively strong, followed by the purification of zinc ferrite, and finally the purchase of zinc ferrite.

It showed from Figure 2(b) that between 200 and 800nm, titanium dioxide and purified zinc ferrite/titanium dioxide composite had certain absorption of light, which was mainly concentrated in the ultraviolet region. When the addition amount (mass fraction) of purified zinc ferrite was 5%, the absorption of titanium dioxide prepared at 400℃ for ultraviolet light was not improved, but the absorption of visible light was improved. The absorption of ultraviolet light and visible light of titanium dioxide prepared at 500℃ was not improved. When the addition of purified zinc ferrite was 10%, the absorption of ultraviolet light was not improved, but the absorption of visible light was improved.

3.3 FT-IR analysis

Figure 3(a) shows the infrared spectrogram of purified zinc ferrite, synthetic zinc ferrite and purchased zinc ferrite. Figure 3(b) shows the infrared spectrogram of titanium dioxide at different calcination temperatures.

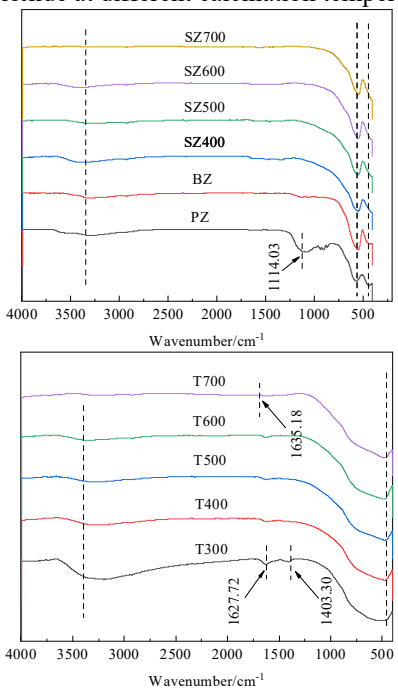

Fig. 3(a) Infrared spectra of different zinc ferrite; (b) Infrared spectra of titanium dioxide at different calcination temperatures

It showed from Figure 3(a) that the positions of characteristic peaks of purified zinc ferrite, synthetic zinc ferrite and purchased zinc ferrite at different calcination temperatures were basically the same. The absorption peaks of the three zinc ferrates near 3383cm^{-1} were caused by the stretching vibrations of the crystal water molecules in the sample, which were generally only involved in metal coordination. In the range of wave number 600~400cm^{-1}, two very obvious absorption characteristic peaks appeared in the purified zinc ferrite, synthetic zinc ferrite and purchased zinc ferrite. The corresponding wave numbers of the two absorption peaks were 570.39cm^{-1} and 433.62cm^{-1} respectively , which were generally considered to be the infrared spectral characteristic peaks of ferrite complex compounds. The absorption peak at 570.39cm^{-1} was due to the vibration of the Zn-O key in the tetrahedral position. The absorption peak of 433.62cm^{-1} was due to the vibration of Fe-O key in octahedral position. In addition, the peak of purified zinc ferrite at 1114.03cm^{-1} was caused by SO_4^{2-} symmetric stretching vibration.

It showed from Figure 3(b) that the absorption peak between 400 and 800cm^{-1} was due to the stretching vibration of Ti-O-Ti bond. The absorption peak between 2950 and 3630cm^{-1} was caused by the expansion of crystal water. In the spectrum of titanium dioxide calcined at 300℃, an absorption peak appeared near 1403.30cm^{-1}

wave number, which was caused by C-H variable angle vibration. In addition, an absorption peak also appeared at 1627.72cm^{-1}, which was caused by the -NH_2 variable angle vibration, which may be due to the low calcination temperature and incomplete volatilization of some organic compounds.

4. Conclusions

(1) In addition to Zn-O, Fe-O bonds and crystal water, SO_4^{2-} also existed in purified zinc ferrite. Zn-O, Fe-O and crystal water appeared in the synthetic zinc ferrite and purchased zinc ferrite, and no other impurity peaks appeared. Purified zinc ferrite, synthetic zinc ferrite, purchased zinc ferrite had different specific surface area, pore volume and average pore size. The specific surface area of purified zinc ferrite was 9.816m$^2\cdot$g^{-1}, that of purchased zinc ferrite was 40.470m$^2\cdot$g^{-1}, and that of synthetic zinc ferrite decreased with the increase of calcination temperature, ranging from 10.686m$^2\cdot$g^{-1} to 35.304m$^2\cdot$g^{-1}. The pore volume of zinc ferrite varied from 0.033cm$^3\cdot$g^{-1} to 0.185cm$^3\cdot$g^{-1}. Their average pore size of the two compounds was less different at about 8nm. The three kinds of zinc ferrite had good absorption to ultraviolet and visible light. The absorption of ultraviolet light by that purified zinc ferrite was the strongest, the absorption of visible light by the synthetic zinc ferrite was relatively the strongest, and the absorption of ultraviolet light and visible light by the purified zinc ferrite was between the two.

(2) The titanium dioxide prepared by chemical coprecipitation method had no other impurity peaks except for Ti-O-Ti bond and crystal water. The specific surface area of titanium dioxide preparation was greatly affected by the calcination temperature. With the increase of calcination temperature, the specific surface area decreased from 123.633 to 28.036m$^2\cdot$g^{-1}. The average pore diameter of titanium dioxide was less affected by calcination temperature and was about 7nm. For the zinc ferrite/titanium dioxide composite prepared by chemical coprecipitation method, a certain amount of purified zinc ferrite was added to facilitate the absorption of visible light by titanium dioxide.

Acknowledgements

The authors would like to acknowledge the financial support received from National Natural Science Foundation of China (No. 52264020, No. 51774099).

References

1. Liu Q. (2020) Pollution and treatment of dye waste-water[C]//IOP Conference Series: Earth and Environmental Science. IOP Publishing, 514(5): 052001.
2. Holkar C R, Jadhav A J, Pinjari D V, et al. (2016) A critical review on textile wastewater treatments: possible approaches[J]. Journal of Environmental Management, 182: 351-366.
3. Han F, Kambala V S R, Srinivasan M, et al. (2009) Tailored titanium dioxide photocatalysts for the degradation of organic dyes in wastewater treatment: A review[J]. Applied Catalysis A: General, 359(1-2): 25-40.
4. Adesanmi B M, Hung Y T, Paul H H, et al. (2022) Comparison of dye wastewater treatment methods: A review[J]. GSC Advanced Research and Reviews, 10(2): 126-137.
5. Weldegebrieal G K. (2020) Synthesis method, antibacterial and photocatalytic activity of ZnO nanoparticles for azo dyes in wastewater treatment: A review[J]. Inorganic Chemistry Communications, 120: 108140.
6. Yu Y, Jimmy C Y, Chan C Y, et al. (2005) Enhancement of adsorption and photocatalytic activity of TiO_2 by using carbon nanotubes for the treatment of azo dye[J]. Applied Catalysis B: Environmental, 61(1-2): 1-11.
7. Rauf M A, Meetani M A, Hisaindee S. (2011) An overview on the photocatalytic degradation of azo dyes in the presence of TiO_2 doped with selective transition metals[J]. Desalination, 276(1-3): 13-27.
8. Ajormal F, Moradnia F, Taghavi Fardood S, et al. (2020) Zinc ferrite nanoparticles in photo-degradation of dye: mini-review[J]. Journal of Chemical Reviews, 2(2): 90-102.